Biosensors and Bioelectronics 126 (2019) 608–614

Contents lists available at ScienceDirect

Biosensors and Bioelectronics

journal homepage: www.elsevier.com/locate/bios

Molecularly imprinted nanoparticles based plasmonic sensors for real-time *Enterococcus faecalis* detection

Özgecan Erdem[a], Yeşeren Saylan[b], Nilüfer Cihangir[a], Adil Denizli[b,*]

[a] Hacettepe University, Department of Biology, 06800, Ankara, Turkey
[b] Hacettepe University, Department of Chemistry, 06800, Ankara, Turkey

ARTICLE INFO

Keywords:
Enterococcus faecalis
Molecular imprinting
Nanoparticle
Sensor

ABSTRACT

Human fecal contamination poses a crucial environmental and health threat in recent years, resulting in the difficulties of access to clean water. According to the World Health Organization, several fecal bacteria, particularly Enterococci species, are present in human intestinal flora. *Enterococcus faecalis* (*E. faecalis*) is one of the indicator bacteria that have been utilized as a pollution indicator in water. However, existing technologies and detection strategies face multiple challenges in terms of low affinity for detection and labelling requirements that limit their access to large scale applications. Here, we present a label-free molecular fingerprinting strategy on a plasmonic sensor to detect *E. fecalis* from aqueous and seawater samples. The kinetic performance of platform was comprehensively evaluated and the platform provided four orders of magnitude detection range with a low limit of detection (down to ~100 bacteria/mL) and a high correlation coefficient value (> 0.99) in the range of 2×10^4–1×10^8 cfu/mL. The platform also denoted a selectivity and specificity while other bacteria (*E. coli*, *B. subtilis*, and *S. aureus*) samples were applied. Multiple time use and relatively long shelf-life are superior to the existing modality. The presented method is one of the fascinating surface modification technique that utilizes biotarget as a recognition element itself, providing a broad range of versatility to replica other biotargets with different molecular structure, size, and physicochemical properties. Such a reliable and versatile platform would hold potential applications from microbiome characterization to forensics by revitalizing obsolescent detection strategies.

1. Introduction

Poor water quality keeps on representing a noteworthy risk for human health in especially developing countries and also accessing to clean drinking water is still a significant limitation on improvement for these countries (Rochelle-Newall et al., 2015). As stated by the World Health Organization, unfortunately almost two billion people use a drinking water source polluted with feces in the world (World Health Organization, 2018). Fecal pollution is the main problem because of the pathogen microorganism spread in water. Different indicator microorganisms such as bacteria, virus, and protozoans are commonly used for determining fecal pollution levels in water (Muniesa et al., 2018). Water resources that utilized for drinking, irrigation, bathing or cooking and can be analyzed for microbiological quality with the detection of fecal indicator bacteria (Martzy et al., 2017). Enterococci are present at high concentration in human and animal intestinal flora and act as indicators of fecal contamination in water. *Enterococcus faecium* and *Enterococcus faecalis* are the most common bacteria in human feces than other *Enterococcus* species. Because of this reason, *Enterococcus faecalis* detection is the topic study of several researchers in the aquatic environment (Boehm and Sassoubre, 2014).

Developing techniques for detection of bacteria species has great significance in different fields including diagnosis of infection diseases, national security, and food safety (Dai et al., 2018; Inci et al., 2013) but well known traditional microorganism detection methods are laborious and time-consuming (Bao et al., 2017). The existing technologies face multiple challenges in terms of low affinity for detection and labelling requirements that limit their access to large scale applications but sensors are employed for the detection of bacteria in recent years. Various sensor types including fluorescence, quartz crystal microbalance, electrochemical and surface plasmon resonance have been utilized for different applications (Saylan et al., 2017a; Battal et al., 2018; Inci et al., 2015). Surface plasmon resonance sensors base on a relation of two main objects (polarized light and metal layer) that measure the refractive index changes in these two layers. The surface plasmon resonance sensors are powerful tools for monitoring of

* Corresponding author.
E-mail address: denizli@hacettepe.edu.tr (A. Denizli).

https://doi.org/10.1016/j.bios.2018.11.030
Received 27 September 2018; Received in revised form 15 November 2018; Accepted 18 November 2018
Available online 19 November 2018
0956-5663/

interactions between different types of molecules (Zeng et al., 2014). Furthermore, specificity, affinity and kinetic parameters during the binding of molecules can be determined in real-time (Saylan et al., 2017c). It is necessary to originate recognition sites on sensor surfaces with high specificity, selectivity, and sensitivity. In recent years, a prominent method called "molecular imprinting" was developed by creating intrinsic cavities of targets into polymeric matrices. Recognition of target is successfully applied in several studies that used for separation, detection and purification with molecular imprinting (Kara et al., 2013; Long et al., 2016). Therefore, the molecularly imprinted polymers can be prepared using the traditional bulk polymerization that has some drawbacks including difficult template removal, slow mass transfer rate, and poor sites accessibility for the template. In order to overcome effectively these drawbacks, the recognition sites must be placed onto or near the substrate surface. Surface imprinting technique is used for macromolecules especially biologically related templates (protein, bacteria, virus etc). Different methods need to be used for creating binding sites on macromolecules surfaces. Important problems in separation as well as sense can be solved with this technique (Ren and Zare, 2012; Schirhagl et al., 2012). The imprinted cavities of the surface molecularly imprinted polymers are distributed in the surface which facilitates the removal and diffusion of templates easily and also enable to develop sensors for microorganism detection. After the removing of the template, the imprinted surface becomes specially functionalized (Hachułka et al., 2010; Saylan et al., 2017d; Li et al., 2014). Besides, new analytical methods are developed to improve the binding kinetics of molecularly imprinted polymers using nanotechnology (Contin et al., 2016; Mazzotta et al., 2016). One of the most important classes of the nanosized structures is that nanoparticles which have high surface-to-volume ratios that increased chemical reactivity, binding capacity, uniform geometry, stability and ease of dispersion, and they provide better accessibility of recognition sites for the targets (Wackerlig and Lieberzeit, 2015). In addition, other properties of nanoparticles such as high electrical conductivity and magnetic property provide several advantages in terms of their usage in imaging, analysis and molecular diagnostic (Sharma et al., 2015).

Due to superior properties of molecularly imprinted nanoparticles compared to bulk materials, they are attractively used for detection with a variety of transducers leading to many sensor types. In this study, we prepare a label-free molecular fingerprinting strategy on a plasmonic sensor to detect *E. fecalis* from aqueous and seawater samples. The polymeric matrices interact with specific amino-acids on bacteria surface antigens, and through these interactions, we achieve to imprint specific regions of bacteria as fingerprints for their detection. This novel plasmonic sensor was developed employing molecularly imprinted nanoparticles that polymerized by amino-acid based monomer for real-time detection of a fecal indicator microorganism, i.e., *E. faecalis*. Followed by the synthesis and characterization of *E. faecalis*-imprinted nanoparticles, the plasmonic sensor was decorated with these *E. faecalis*-imprinted nanoparticles and then characterized through ellipsometry and contact angle measurements. As a control, the non-imprinted plasmonic sensor was also fabricated using non-imprinted nanoparticles which have no *E. faecalis*. Benchmarking kinetic analyses, selectivity and repeatability performances of the plasmonic sensors were comprehensively evaluated through the real-time detection of *E. faecalis*. Further, the *E. faecalis*-imprinted plasmonic sensor was validated with seawater samples.

2. Experimental

2.1. Materials

Enterococcus faecalis (ATCC® 29212™), *Escherichia coli* (*E. coli*, ATCC® 11303™), *Staphylococcus aureus* (*S. aureus*, ATCC® 14990™) and *Bacillus subtilis* subsp. *subtilis* (*B. subtilis*, ATCC® 6051™) were obtained from American Type Culture Collection (ATCC), USA. Phosphate buffer saline (PBS), Luria Bertani (LB) and Trypticase Soy Broth (TSB) were purchased from Fisher Scientific Co. (New Jersey, USA) and Pronadisa (Madrid, Spain). Poly vinyl alcohol (PVA), sodium dodecyl sulfate (SDS), sodium bicarbonate ($NaHCO_3$), 2-hydroxyethyl methacrylate (HEMA), ethylene glycol dimethacrylate (EGDMA), sodium bisulfite ($NaHSO_3$) and ammonium persulfate ($(NH_4)_2S_2O_8$) were obtained from Sigma-Aldrich Corporation (MO, USA). Amino-acid based monomer, N-methacryloyl-(L)-histidine-methylester (MAH), was synthesized as previously described (Garipcan and Denizli, 2002). The gold coated surfaces were purchased from GWC Technologies (WI, USA).

2.2. Preparation of bacteria

E. faecalis and another competitor bacteria (*S. aureus, B. subtilis, and E. coli)* were inoculated into the TSB and LB broth medium. They incubated under static conditions at 37 °C for 18 h. Then, serial 10-fold dilutions of each bacterium were prepared and 100 µL of aliquots of each dilution were plated onto agar and incubated again for at 37 °C 18 h. The concentrations of each bacterium were calculated as colony forming unit per mL (cfu/mL) after incubation. 1 mL of each bacterium were centrifuged at 6000 rpm for 15 min and bacteria pellet was re-suspended with PBS (pH 7.4) six times in order to wash away the growth medium. Finally, the *E. faecalis* suspension was prepared with sterile PBS solution. The suspension was used for the preparation of *E. faecalis*-imprinted nanoparticles and kinetic analyses of the *E. faecalis*-imprinted plasmonic sensor. The glycerol stocks of each bacterium were placed at − 80 °C separately for later use. Each solution was prepared with fresh culture and stored at + 4 °C until used.

2.3. Preparation and characterization of the E. faecalis-imprinted nanoparticles

E. faecalis-imprinted nanoparticles were prepared by the following procedure as described in a previous study (Saylan et al., 2015e): The amino-acid based monomer, N-methacryloyl-(L)-histidine-methylester called as MAH and *E. faecalis* were mixed to form a pre-complex for an hour before polymerization. Two phases emulsion method was used in order to prepare *E. faecalis*-imprinted nanoparticles. The first phase was prepared by dissolving of poly vinyl alcohol (PVA) and sodium dodecyl sulfate (SDS) as a stabilizer and surfactant to form an emulsion. Sodium bicarbonate ($NaHCO_3$) was used as an agent in order to adjust pH in water. PVA and SDS were also used for the purpose of preparing the second phase. The second phase was a monomer phase, which consisted of 2-hydroxyethyl methacrylate (HEMA) and ethylene glycol dimethacrylate (EGDMA) acted as a co-monomer and cross-linker, was added to the first phase and homogenized at 6000 rpm by a homogenizer (T10, Ika Labortechnik, Germany) in 30 min to obtain an emulsion. The pre-complex was added to a mixture and then the final mixture was transferred to a polymerization system. Sodium bisulfite ($NaHSO_3$) and ammonium persulfate ($(NH_4)_2S_2O_8$) were added to the final mixture as initiators and the polymerization was carried out at 40 °C for 24 h, with mechanically stirring at 500 rpm (Scheme 1). This condition did not hinder bacteria growth as indicated in the literature (Fisher and Phillips, 2009). The non-imprinted nanoparticles were also synthesized with the same procedure except using the *E. faecalis*. The *E. faecalis*-imprinted and non-imprinted nanoparticles washed with ethanol, water-ethanol mixture and water in several times using centrifugation at 30000 rpm for 45 min (Allegra-64R Beckman Coulter, USA). As a desorption agent, 0.1 M NaCl solution was used for the removal of *E. faecalis* from the *E. faecalis*-imprinted nanoparticles. The desorption process was continued until no absorbance observation at 600 nm by UV–visible spectrophotometry (McBirney et al., 2016). After washing steps, *E. faecalis*-imprinted nanoparticles were dispersed in ultra-pure water and kept at 4 °C until use.

In order to characterize the *E. faecalis*-imprinted nanoparticles, size distribution, chemical structure and surface morphology was examined

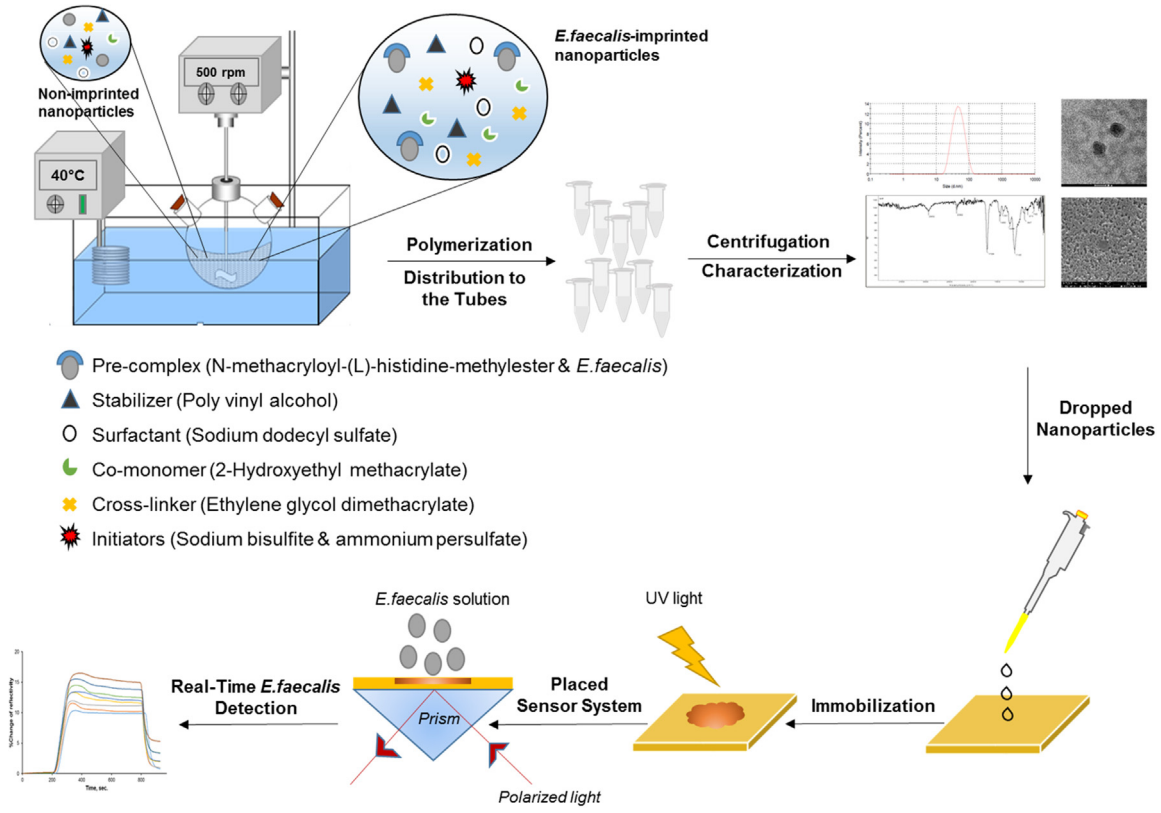

Scheme 1. The preparation of *E. faecalis*-imprinted plasmonic sensor.

using a ZetaSizer Nano-ZS (Malvern Instrument Company, UK) and Fourier transform infrared (FTIR) spectroscopy (Thermo Fisher Scientific, Nicolet iS10, Waltham, MA, USA), scanning electron microscopy (SEM, Quanta 400F Field Emission, USA) and transmission electron microscopy (TEM, FEI/Tecnai G^2 Spirit Biotwin, USA).

2.4. Preparation and characterization of the plasmonic sensors

10 μL of *E. faecalis*-imprinted and non-imprinted nanoparticle solution was dropped onto the plasmonic sensor surfaces and were coated equally by the spin-coating system. The immobilizations were carried out under ultraviolet (UV) light (100 W, 365 nm) for 30 min. The plasmonic sensors were incubated in an oven overnight at 40 °C to only stabilize immobilization. An ellipsometry (Nanofilm EP3, Germany) measured the thickness of the plasmonic sensor surfaces and drope shape analyzer (KRUSS, DSA100, Germany) was also employed to determine the hydrophilicity of the plasmonic sensor surfaces. The contact angle values were determined and calculated with the sessile drop method in an average of three water drops.

2.5. Kinetic analyses of the plasmonic sensors

Followed by characterization experiments, *E. faecalis*-imprinted and non-imprinted plasmonic sensors were individually used by SPRimager II (GWC Technologies, US). At first, the plasmonic sensor was washed and equilibrated with ultrapure water and then PBS (pH 7.4) with the same flow rate (150 μL/min) in each experiment. The resonance angle was adjusted with the mirror and all the analyses were performed at this same angle. Repeatedly, the buffer motion continued with a pump for 180 s to obtain a baseline. The volume of the sample solutions was adjusted to 5 mL and each sample solutions were applied to the surface plasmon resonance system one by one. The changes of reflectivity values were monitored and reached a plateau value in 780 s for each sample solution. After that, 0.1 M NaCl solution was used in the desorption process. The plasmonic sensors were cleaned up with water by PBS afterward. The flow rate was the same in all experiments. Different concentrations of *E. faecalis* solutions (2×10^4–1×10^8 cfu/mL) were utilized for the benchmarking kinetic analyses and interacted with the *E. faecalis*-imprinted plasmonic sensor. The real-time responses of the plasmonic sensors were saved at the end of each analysis.

2.6. Selectivity and repeatability analyses of the plasmonic sensors

The plasmonic sensors also denoted a selectivity and specificity while other bacteria (*E. coli, B. subtilis*, and *S. aureus*) samples were applied. *E. coli, B. subtilis,* and *S. aureus* sample solutions were prepared with the same concentration (2×10^5 cfu/mL) and interacted with *E. faecalis*-imprinted and non-imprinted plasmonic sensors individually to compare the selectivity behavior. Furthermore, the different concentrations of *E. faecalis* sample solutions (2×10^5, 2×10^6, 2×10^7 and 2×10^8 cfu/mL) were applied to the non-imprinted plasmonic sensor to observe real-time responses and compare these responses of *E. faecalis*-imprinted and non-imprinted plasmonic sensors. According to analyses, selectivity and relative selectivity coefficients were also calculated to discuss in detail of this parameter. Multiple time use and relatively long shelf-life were superior to the existing modality. For this purpose, a same *E. faecalis* sample solution (1×10^5 cfu/mL) was interacted four times to test the repeatability performance of the *E. faecalis*-imprinted plasmonic sensor.

2.7. Real sample analyses

The real sample, seawater (Marmara Sea, Turkey), which could provide an available medium for bacteria growth and one of the significant potential pollution sources among various factors such as recreational, domestic and industrial activities was interacted with the *E. faecalis*-imprinted plasmonic sensor to observe the response in complex medium. Seawater sample was diluted 10 times with PBS and then

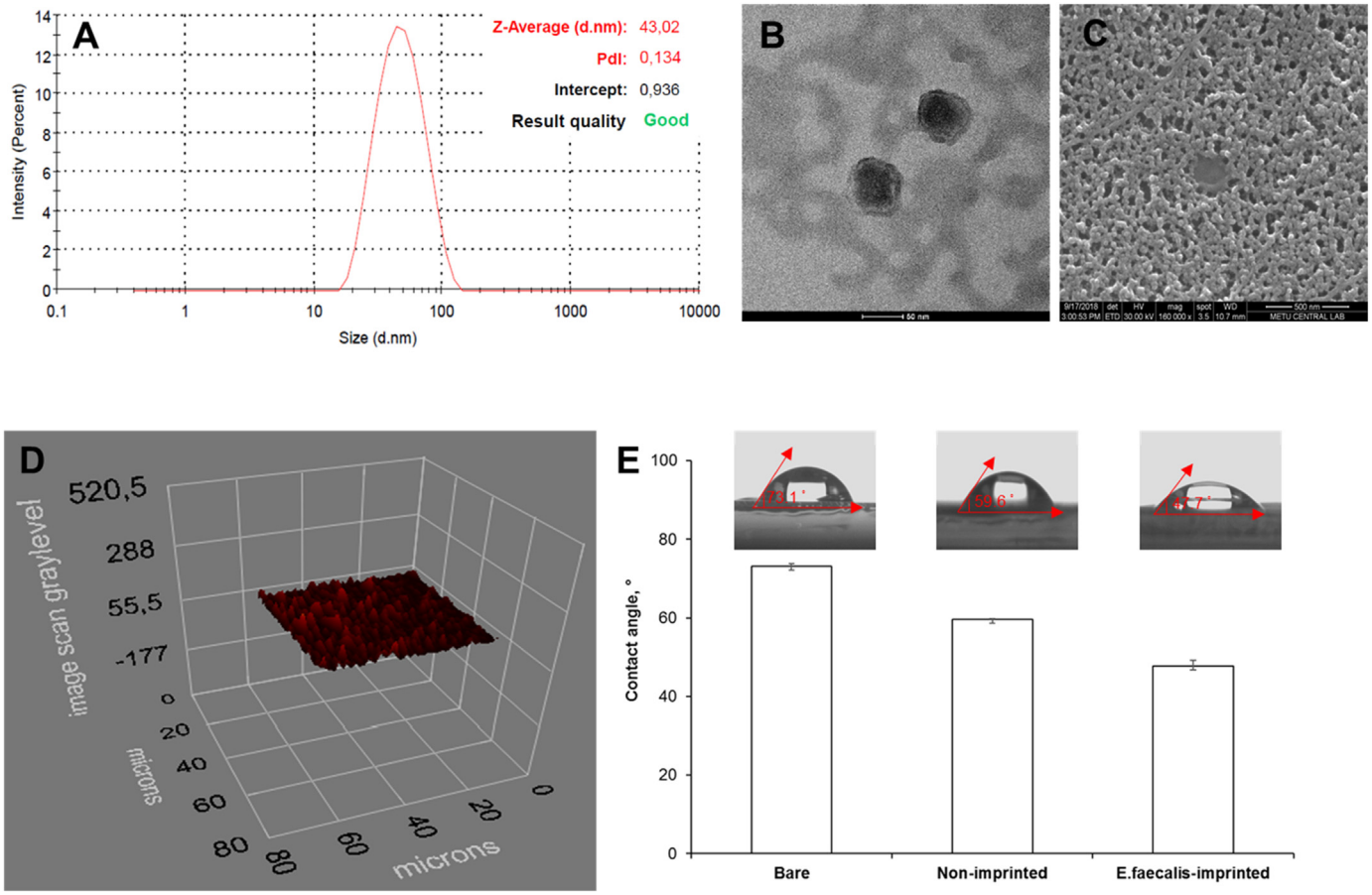

Fig. 1. Characterization analyses of the *E. faecalis*-imprinted nanoparticles and plasmonic sensors: Particle size distribution (A), TEM (B), SEM (C), ellipsometry (D) images and contact angle results (E).

spiked with *E. faecalis* as the bacteria concentrations would be 1×10^6, 1×10^7 and 1×10^8 cfu/mL, separately (İdil et al., 2017).

3. Results and discussion

3.1. Characterization analyses

Characterization analyses were carried out by zeta-size, FTIR, SEM, TEM, ellipsometry and contact angle measurements. The average particle size of *E. faecalis*-imprinted nanoparticles was measured as around 43 nm with 0.134 polydispersity index (Fig. 1A). According to the TEM and SEM analyses, the *E. faecalis*-imprinted nanoparticles had very close (~ 50 nm) size to the zeta-size analysis, spherical shapes and rough surfaces (Figs. 1B–C). The surface imprinting technique was employed to imprint bacteria. So, the size of nanoparticles was measured as nanometer scales. The functional groups of amino-acid based monomer had a peak at around 1640 cm^{-1} and 1460 cm^{-1} that assigned the amide I and amide II stretching vibration bands and also a sharp peak at 1730 cm^{-1} assigned the ester band in FTIR spectrum and shown in Fig. S1 (Saylan et al., 2017b). In addition, the ellipsometry analysis of the *E. faecalis*-imprinted plasmonic sensor reflected that it had a rough surface due to the immobilization of the nanoparticles and the thickness of *E. faecalis*-imprinted plasmonic sensor was measured as 70.8 ± 6.0 nm, respectively (Fig. 1D). Finally, the contact angle value of the *E. faecalis*-imprinted plasmonic sensor was decreased from 73.1° ± 0.69 to 47.7° ± 1.47 by modifying bare sensor surface with nanoparticle immobilization due to the increase of hydrophilicity of the sensor surface by presenting amide groups of amino-acid based monomer (Fig. 1E).

3.2. Kinetic analyses

Following the characterization analyses, the *E. faecalis*-imprinted plasmonic sensor was employed for real-time detection of *E. faecalis* from aqueous solutions. For this purpose, *E. faecalis*-imprinted plasmonic sensor interacted with *E. faecalis* sample solutions in the range from 2×10^4 to 1×10^8 cfu/mL. As shown in Fig. 2A, the *E. faecalis*-imprinted plasmonic sensor had a prompt response (45 s) when the *E. faecalis* solutions arrived at the plasmonic sensor surface. The increase of *E. faecalis* concentration caused an increase in plasmonic sensor response. After the saturation point, the *E. faecalis*-imprinted plasmonic sensor was treated with 0.1 M NaCl and then ultrapure water to inject next *E. faecalis* solution into the sensor system.

The bacteria adhesion to a surface occurs with various physicochemical interactions (Hamadi et al., 2008; Yilmaz et al., 2015). Further, *E. faecalis* is a Gram positive bacteria and carries a negative charge due to the presence of teichoic acid in the peptidoglycan located on the outer membrane (Tokonami et al., 2014). In the process of nanoparticle preparation, an amino-acid (histidine) based monomer was used, and its carboxyl, imidazole and amino groups interacted with *E. faecalis* at around their isoelectric points (Garipcan and Denizli, 2002). As histidine is positively charged, it interacts with the negatively charged bacteria surface at pH 7.4. So, the interaction occurred between these functional groups of monomer and L-lysin and glutamic acid residues of *E. faecalis* (Perçin et al., 2017).

According to the results, there is a straight relation between the *E. faecalis* solutions' concentration and change of reflectivities of the plasmonic sensor. Further examinations on the performance of *E. faecalis*-imprinted plasmonic sensor denoted 99.2% precision for *E. faecalis* concentrations from 2×10^4 to 1×10^8 cfu/mL (Fig. 2B). The *E.*

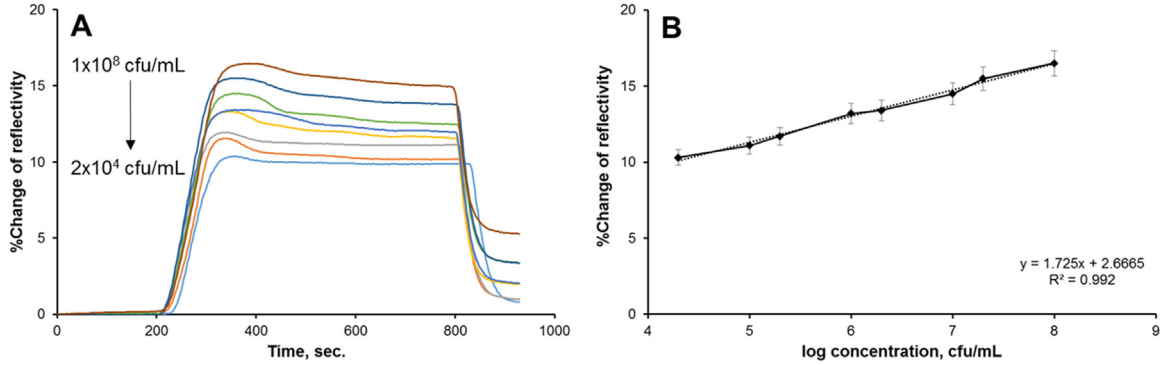

Fig. 2. The real-time *E. faecalis* detection (A) and relationship between the change of reflectivities and logarithm of *E. faecalis* concentrations (B).

faecalis-imprinted plasmonic sensor response (y) is linearly associated with *E. faecalis* solutions' concentration (x). It can be stated as $y = a + bx$ for a calibration curve. This can be used for determining the limit of detection and quantification values. Hence, the limit of detection and quantification values can be also stated as 3 s/b and 10 s/b where s is the standard deviation of the *E. faecalis*-imprinted plasmonic sensor response can be evaluated by s of either y-intercept of regression lines (Dibekkaya et al., 2016). A homogeneous distribution occurred in a more relevant assessment and the limit of detection and quantification values were calculated as 1.05×10^2 cfu/mL and 3.5×10^2 cfu/mL for *E. faecalis*-imprinted plasmonic sensor. So, the *E. faecalis*-imprinted plasmonic sensor provided four orders of magnitude detection range with a low limit of detection (down to ~100 bacteria/mL) and a high correlation coefficient value (> 0.99) in the range of 2×10^4–1×10^8 cfu/mL.

3.3. Selectivity and repeatability analyses

Structurally related bacteria, *E. coli, B. subtilis,* and *S. aureus,* were used as competitor agents for comparison the selectivity behaviors of the *E. faecalis*-imprinted and non-imprinted plasmonic sensors. *E. coli* was selected for differences in Gram and morphological properties while *B. subtilis* was selected for Gram property similarity and *S. aureus* both Gram and morphological similarities. Fig. 3A reflected that the *E. faecalis*-imprinted plasmonic sensor had different responses to different bacteria. Also, the non-imprinted plasmonic sensor interacted with several *E. faecalis* sample solutions (2×10^5, 2×10^6, 2×10^7 and 2×10^8 cfu/mL) to compare responses of for control experiments (Fig. S2A). As demonstrated in Fig. S2B, the non-imprinted plasmonic sensor has very low capability to detect *E. faecalis.* According to the calibration curves and slopes of *E. faecalis*-imprinted and non-imprinted plasmonic sensors, the *E. faecalis*-imprinted plasmonic sensor was more selective than the non-imprinted plasmonic sensor (Fig. S2C). All selectivity and relative selectivity coefficients for the *E. faecalis*-imprinted and non-imprinted plasmonic sensors were also given in Table S1. Combining advantages of molecular imprinting and nanoparticle promoted both sensitivity and selectivity for the detection of *E. faecalis*. In literature, the selectivity and relative selectivity coefficients are ≥ 2 considered to be satisfactory for molecularly imprinted systems. It means that selectivity of an imprinted polymer is estimated by means of the selectivity factor, which reflects the selectivity of binding of the target molecule by the imprinted polymer with respect to the selectivity of binding of structural analogues of the template used to form the imprint sites (Chen et al., 2016; Shumyantseva et al., 2016; Vlakh et al., 2015; Zhang et al., 2014).

The repeatability performance of the *E. faecalis*-imprinted plasmonic sensor was tested using the same *E. faecalis* solution (1×10^5 cfu/mL) in four adsorption-desorption cycles. As seen in Fig. 3B, the change of reflectivity of *E. faecalis*-imprinted plasmonic sensor was decreased from 11.06% to 10.63% and there was only 0.43% lost of performance. The results showed that *E. faecalis*-imprinted plasmonic sensor can be used for *E. faecalis* detection several times without any performance lost. So, multiple time use and relatively long shelf-life are superior to the *E. faecalis*-imprinted plasmonic sensor.

3.4. Real sample analyses

Real sample analyses were performed to investigate the real-time applicability of *E. faecalis*-imprinted plasmonic sensor in a different medium. Fig. 4 demonstrated that the change of reflectivity value increase caused by the increase *E. faecalis* concentration in seawater sample. In other words, the *E. faecalis*-imprinted plasmonic sensor was capable to detect *E. faecalis* with a recovery of 92–98% with different concentration of *E. faecalis* samples with the relative standard deviation

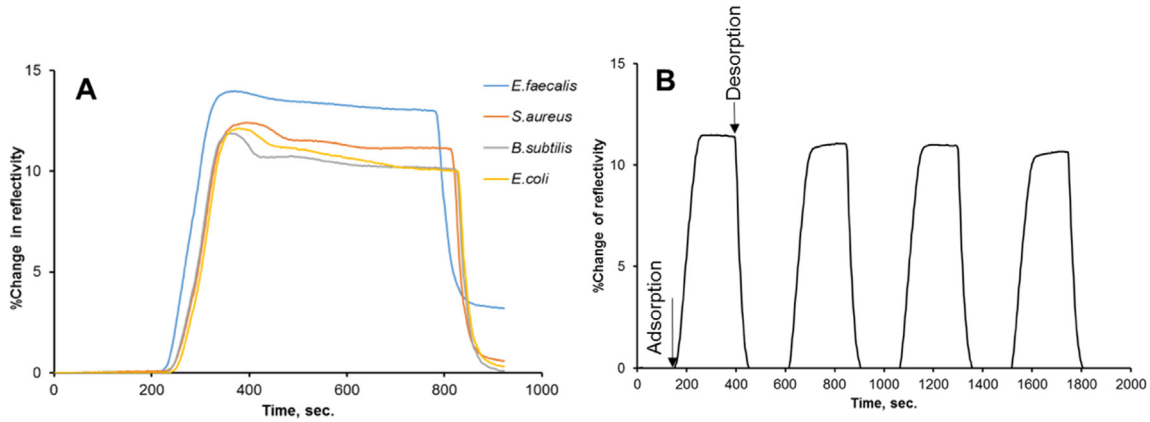

Fig. 3. Selectivity (A) and repeatability (B) of the *E. faecalis*-imprinted plasmonic sensor.

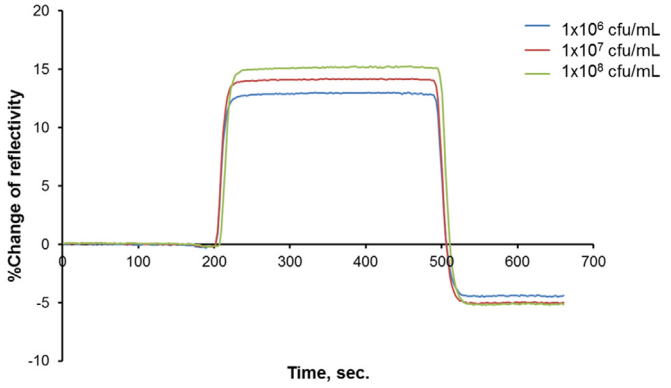

Fig. 4. Real-time responses of the *E. faecalis*-imprinted plasmonic sensor in seawater.

values (3.55, 2.34 and 3.46) and also negative change of reflectivity values were observed after desorption agent applied due to non-specific interaction of other components of the seawater.

Table 1 was prepared to summarize of different imprinting methods for several types of bacteria detecting in a broad detection range. According to the comparison, the researchers chose structurally related bacteria for selectivity studies and also some of them performed real sample experiments by using a different medium. Furthermore, distinct bacteria have different surface antigens, and their capture efficiency performance differed that we presented for *E. faecalis*. In our study, we reported a label-free molecular fingerprinting strategy on a plasmonic sensor to detect E. fecalis from aqueous and seawater samples. This paper is the first study, which is the integration of *E. faecalis*-imprinted nanoparticles to the plasmonic sensors for real-time detection of *E. faecalis*. The large surface area offered by molecularly imprinted nanoparticles presented more binding sites, which will drive the great development of molecularly imprinted polymers with other promising applications to detect different bacteria. Such a reliable and versatile platform will hold potential applications from microbiome characterization to forensics by revitalizing obsolescent detection strategies.

4. Conclusions

Fecal contamination of drinking water creates an important and a crucial health and environmental threat in recent years due to the difficulties of access to clean water. Due to these reasons, detection of pollution with the bacteria is necessary. Here, *E. faecalis*-imprinted nanoparticles were first synthesized and then integrated onto plasmonic sensors for real-time *E. faecalis* detection in both aqueous and real sample solutions. The kinetic performance of *E. faecalis*-imprinted plasmonic sensor was comprehensively evaluated and the *E. faecalis*-imprinted plasmonic sensor provided four orders of magnitude detection range with a low limit of detection and a high correlation coefficient value. Further, the selectivity analyses showed that the specific cavities of the *E. faecalis*-imprinted plasmonic sensor much more recognized *E. faecalis* than other competitors. The presented method is one of the fascinating surface modification technique that utilizes target as a recognition element itself, providing a broad range of versatility to replica other targets with different molecular structure, size, and physicochemical properties. In the light of the obtained data, the plasmonic sensor can be employed as a possible option to detect other bacteria and used for the environment and human health protection. Besides some disadvantages including morphology and size of bacteria and the low refractive index contrast between the cytoplasm of microorganism and the environment, sensor technology is still an easy-to-use method for microorganism detection. Developing a portable sensor for in situ detection of microorganisms and making it available for environmental pollution control is among our future research.

Table 1
Summary of different methods for bacteria detection.

Method	Type of bacteria	Detection range	Limit of detection	Selectivity	Real sample	Reference
Micro-contact imprinting	*S. paratyphi*	2.5–15 × 10^6 cfu/mL	1.4 × 10^6 cfu/mL	*E. coli, S. aureus, B. subtilis*	Apple juice	Perçin et al. (2017)
Micro-contact imprinting	*E. coli*	0.5–4.0 McFarland	1.54 × 10^6 cfu/mL	*S. aureus, B. subtilis*	Apple juice	Yılmaz et al. (2015)
Immobilized bacteriophage	*E. coli*	7 × 10^2–7 × 10^8 cfu/mL	7 × 10^7 cfu/mL	*E. coli*	Not available	Arya et al. (2011)
Bacteriophage	*Salmonella*	10^6–10^9 cfu/mL	8 × 10^7 cfu/mL	*L. monocytogenes, E. coli, Salmonella*	Not available	Karoonuthaisiri et al. (2014)
Immobilized mannose	*E. coli*	1.0–10^{11} cfu/mL	3.0 cfu/mL	*C. freundii, S. epidermidis*	Spinach leaves	Yazgan et al. (2014)
Micro-contact imprinting	*E. coli*	10^2–10^7 cfu/mL	70 cfu/mL	*B. subtilis, S. aureus S. paratyphi*	River water, apple juice	İdil et al. (2017)
Cell-imprinted polymer	*S. epidermidis*	10^3–10^7 cfu/mL	Not available	*D. proteolyticus, E. coli, S. pneumoniae*	Not available	Golabi et al. (2017)
Spore-imprinted polymer	*Bacillus cereus* spores	10^2–10^5 cfu/mL	10^2 cfu/mL	*B. subtilis* spores	Not available	Lahcen et al. (2018)
Molecularly imprinted nanoparticle	***E. faecalis***	**2 × 10^4 – 1 × 10^8 cfu/mL**	**1.05 × 10^2 cfu/mL**	***E. coli, B. subtilis, S. aureus***	**Seawater**	**This study**

Acknowledgements

This work was supported by Hacettepe University Scientific Research Projects Coordination Unit, Ankara, Turkey (No. FBA-2017-13815).

Appendix A. Supporting information

Supplementary data associated with this article can be found in the online version at doi:10.1016/j.bios.2018.11.030.

References

Arya, S.K., Singh, A., Naidoo, R., Wu, P., McDermott, M.T., Evoy, S., 2011. Analyst 136, 486–492.
Bao, H., Yang, B., Zhang, X., Lei, L., Li, Z., 2017. Chem. Commun. 53, 2319–2322.
Battal, D., Akgönüllü, S., Yalcin, M.S., Yavuz, H., Denizli, A., 2018. Biosens. Bioelectron. 111, 10–17.
Boehm, A.B., Sassoubre, L.M., 2014. Enterococci as indicators of environmental fecal contamination, in: Gilmore, M. S., Clewell, D. B., Ike, Y., Shankar, N. (Eds.). Enterococci: From Commensals to Leading Causes of Drug Resistant Infection, pp. 101–121.
Chen, L., Wang, X., Lu, W., Wu, X., Li, J., 2016. Chem. Soc. Rev. 2016 (45), 2137–2213.
Contin, M., Bonelli, P., Lucangioli, S., Cukierman, A., Tripodi, V., 2016. J. Chromatogr. A 1456, 1–9.
Dai, B., Wang, L., Wang, Y., Yu, G., Huang, X., 2018. Chem. Sel. 3 (25), 7208–7221.
Dibekkaya, H., Saylan, Y., Yılmaz, F., Derazshamshir, A., Denizli, A., 2016. J. Macromol. Sci. Part A Pure Appl. Chem. 53 (9), 585–594.
Fisher, K., Phillips, C., 2009. Microbiology 155 (6), 1749–1757.
Garipcan, B., Denizli, A., 2002. Macromol. Biosci. 2, 135–144.
Golabi, M., Kuralay, F., Jager, E.W., Beni, V., Turner, A.P., 2017. Biosens. Bioelectron. 93, 87–93.
Hachułka, K., Lekka, M., Okrajni, J., Ambroziak, W., Wandelt, B., 2010. Biosens. Bioelectron. 26 (1), 50–54.
Hamadi, F., Latrache, H., Zahir, H., Elghmari, A., Timinouni, M., Ellouali, M., 2008. Braz. J. Microbiol. 39, 10–15.
Idil, N., Hedström, M., Denizli, A., Mattiasson, B., 2017. Biosens. Bioelectron. 87, 807–815.
Inci, F., Tokel, O., Wang, S., Gurkan, U.A., Tasoglu, S., Kuritzkes, D.R., Demirci, U., 2013. ACS Nano 7 (6), 4733–4745.
Inci, F., et al., 2015. Proc. Natl. Acad. Sci. USA 112 (32), E4354–E4363.
Kara, M., Uzun, L., Kolayli, S., Denizli, A., 2013. J. Appl. Polym. Sci. 129, 2273–2279.
Karoonuthaisiri, N., Charlermroj, R., Morton, M.J., Oplatowska-Stachowiak, M., Grant, I.R., Elliott, C.T., 2014. Sens. Actuators B-Chem. 190, 214–220.
Lahcen, A.A., Arduini, F., Lista, F., Amine, A., 2018. Sens. Actuator B-Chem. 276, 114–120.
Li, S., Cao, S., Whitcombe, M.J., Piletsky, S.A., 2014. Prog. Polym. Sci. 39 (1), 145–163.
Long, Y., Li, Z., Bi, Q., Deng, C., Chen, Z., Bhattachayya, S., Li, C., 2016. Int. J. Pharm. 502, 232–241.
Martzy, R., Kolm, C., Brunner, K., Mach, R.L., Krska, R., Šinkovec, H., Sommer, R., Farnleitner, A.H., Reischer, G.H., 2017. Water Res. 122, 62–69.
Mazzotta, E., Turco, A., Chianella, I., Guerreiro, A., Piletsky, S.A., Malitesta, C., 2016. Sens. Actuators B-Chem. 229, 174–180.
McBirney, S.E., Trinh, K., Wong-Beringer, A., Armani, A.M., 2016. Biomed. Opt. Express 7 (10), 4034–4042.
Muniesa, M., Ballesté, E., Imamovic, L., Pascual-Benito, M., Toribio-Avedillo, D., Lucena, F., Blanch, A.R., Jofre, J., 2018. Water Res. 128, 10–19.
Perçin, I., Idil, N., Bakhshpour, M., Yılmaz, E., Mattiasson, B., Denizli, A., 2017. Sensor 17, 1375–1388.
Ren, K., Zare, R.N., 2012. ACS Nano 6 (5), 4314–4318.
Rochelle-Newall, E., Nguyen, T.M.H., Le, T.P.Q., Sengtaheuanghoung, O., Ribolzi, O., 2015. Front. Microbiol. 6 (308), 1–15.
Saylan, Y., Akgönüllü, S., Çimen, D., Derazshamshir, A., Bereli, N., Yılmaz, F., Denizli, A., 2017a. Sens. Actuators B-Chem. 241, 446–454.
Saylan, Y., Tamahkar, E., Denizli, A., 2017b. J. Biomater. Sci. Polym. Ed. 28, 1950–1965.
Saylan, Y., Yılmaz, F., Derazshamshir, A., Yılmaz, E., Denizli, A., 2017c. J. Mol. Recognit. 30, 1–7.
Saylan, Y., Yilmaz, F., Özgür, E., Derazshamshir, A., Yavuz, H., Denizli, A., 2017d. Sensor 17 (4), 898–928.
Saylan, Y., Uzun, L., Denizli, A., 2015e. Ind. Eng. Chem. Res. 54, 454–461.
Schirhagl, R., Ren, K., Zare, R.N., 2012. Sci. China Chem. 55 (4), 469–483.
Sharma, R., Ragavan, K.V., Thakur, M.S., Raghavarao, K.S.M.S., 2015. Biosens. Bioelectron. 74, 612–627.
Shumyantseva, V.V., Bulko, T.V., Sigolaeva, L.V., Kuzikov, A.V., Archakov, A.I., 2016. Biosens. Bioelectron. 86, 330–336.
Tokonami, S., Nakadoi, Y., Nakata, H., Takami, S., Kadoma, T., Shiigi, H., Nagaoka, T., 2014. Res. Chem. Intermed. 40, 2327–2335.
Vlakh, E.G., Korzhikov, V.A., Hubina, A.V., Tennikova, T.B., 2015. Russ. Chem. Rev. 84, 952–980.
Wackerlig, J., Lieberzeit, P.A., 2015. Sens. Actuators B-Chem. 207, 144–157.
World Health Organization, 2018. WHO-Drinking water [WWW Document]. URL 〈http://www.who.int/mediacentre/factsheets/fs391/en/〉 (Accessed 22 February 2018).
Yazgan, I., Noah, N.M., Toure, O., Zhang, S., Sadik, O.A., 2014. Biosens. Bioelectron. 61, 266–273.
Yilmaz, E., Majidi, D., Ozgur, E., Denizli, A., 2015. Sens. Actuators B-Chem. 209, 714–721.
Zhang, et al., 2014. Anal. Chem. 463, 7–14.
Zeng, S., Baillargeat, D., Ho, H.-P., Yong, K.-T., 2014. Chem. Soc. Rev. 43, 3426–3452.